ELSEVIER

Off-line LDI-TOF-MS monitoring of simultaneous inorganic and organic reactions on particles levitated in a laboratory environment

Allen E. Haddrell, Xiao Feng, Ray Nassar, Michael J. Bogan,
George R. Agnes*

*Department of Chemistry, Simon Fraser University, 8888 University Drive, Burnaby, B.C.,
Canada V5A 1S6*

Abstract

Simultaneous inorganic and organic reactions occur on tropospheric particles. The outcomes of these parallel reaction pathways, and particularly the minor reaction products that collectively sum to an appreciable fraction of the particle's mass, are the focus of this work. To characterize condensed phase organic, inorganic, and metal-organic reaction products, we are developing methodology that involves, firstly, the creation of picoliter droplets that carry net charge that are trapped and levitated by an electrodynamic balance in a laboratory environment for the duration of the experiment. Following the rapid evaporation of volatile solvents from the droplets (i.e. seconds), either a residual droplet or a particle remains levitated depending on the atmospheric conditions inside the levitation chamber and the composition of the starting solution from which the initial droplets were created. These droplet residues, whose initial composition is known, are then exposed to gaseous compounds and oxidants that cause transformation of the composition of the levitated droplets/particles by multiphase and heterogeneous reactions that proceed dependent on the species condensing and reacting on the particles. The droplets/particles are then deposited onto a substrate that allows subsequent, and detailed characterization by instrumental methods. In the studies reported here, laser desorption ionization time of flight mass spectrometry was used to characterize reaction products that had formed on the levitated droplets/particles. This apparatus and methodology were used to study the effect of the inorganic reaction of nitric acid vapor with $NaCl_{(aq)}$ and $NaCl_{(s)}$ on the formation of imines by dehydration reaction between

---

* Corresponding author. Tel.: +1 604 291 4387; fax: +1 604 291 3765.
  E-mail address: gagnes@sfu.ca (G.R. Agnes).

the functional groups of a primary amine and an aldehyde. The product yield of imines was found to be dependent on the sequence of introduction of the gaseous reactants to the levitation chamber.

1. Introduction

Collectively, particles suspended in the troposphere are involved in atmospheric processes that influence climate, such as cloud formation, light absorption and scattering, and visibility reduction. (Finlayson-Pitts & Hemminger, 2000; Finlayson-Pitts & Pitts, 1997). In addition, the composition of suspended particles is believed to determine health outcomes following inhalation exposure (Adamson, Prieditis, & Vincent, 1999; Dockery, Pope, & Xu, 1993; Pope et al., 1995; Salvi & Holgate, 1999; Samet, Dominici, Curriero, Coursac, & Zeger, 2000; Somers, McCarry, Malek, & Quinn, 2004; Tan et al., 2000; van Eeden et al., 2001; Vincent et al., 1997; Willerson & Ridker, 2004). Improved characterization of individual particle composition, and the reactions involved in their transformations could lead to effective strategies that mitigate the adverse effects on climate and on human health from inhalation exposure to suspended particles (Brook et al., 2004).

The chemical composition of the particulate matter suspended in the troposphere is representative of its formation processes as well as its chemical alteration within the troposphere through homogeneous, heterogeneous and multiphase reactions during its lifetime (Ravishankara, 1997; Zenobi, Haefliger, & Bucheli, 2000). Particle cores range from inorganic wind blown dusts and sea spray to purely organic particle cores in secondary organic aerosols, or both, as found in carbonaceous particles derived from high temperature combustion sources. These particles also contain varied quantities of water, inorganic (nitrates and sulfates) and organic compounds depending on the airmass and the local environmental conditions. Particle phase reactions that proceed by heterogeneous and multiphase pathways have been implicated between the reactive functional groups of oxidized organic compounds, in the formation of polymeric compounds (Jang, Czoschke, Lee, & Kamens, 2002; Kalberer et al., 2004) and on the involvement of radicals initiated by attack from tropospheric oxidants in the further transformation of a particle's composition. In addition to those reactions whose product yields are the subject of current investigation, many other compounds generated at low absolute yields that could be toxic to human lung cells are expected. Metal organic compounds, for instance, could be produced within the films that coat suspended particles in the troposphere and the toxicity of such compounds are poorly characterized.

Here we report a laboratory apparatus and associated methodology (Fig. 1) that will be applied to the study of parallel organic, inorganic, and metal-organic reactions on suspended particles. We utilize particle levitation technology (Schweiger & Davis, 2002; Aardahl, Vehring, Davis, Schweiger, & Swanson, 1997; Davis, 1997; Vehring, Aardahl, Davis, Schweiger, & Covert, 1997; Wuerker, Shelton, & Langmuir, 1959) with methodology developed by our group to extract a synthesized particle from a controlled atmosphere in a levitation chamber and cause it to impact onto a stainless steel plate (Bogan & Agnes, 2002). That last step is key to our methodology because the deposition of individual particles onto separate locations on a deposition plate allows a number of instrumental techniques to be utilized in the identification of the compounds on each particle, the distribution of these compounds within each particle, and their relative abundance. Here we demonstrate the potential of this apparatus by introducing high concentrations of nitric acid and aldehyde vapors into a chamber in which NaCl containing droplets and NaCl particles were
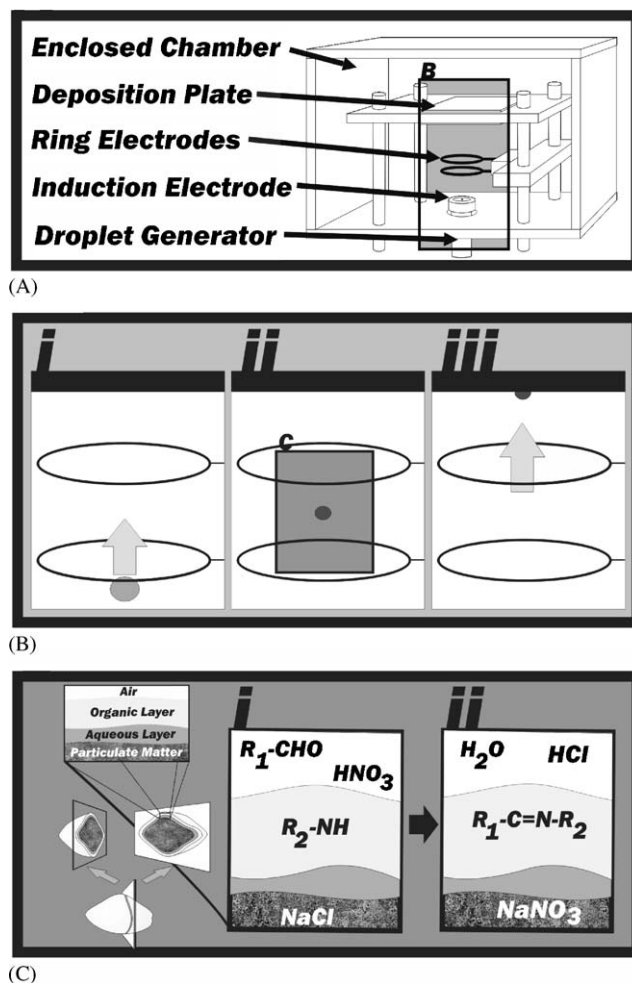
Fig. 1. A pictorial summary of the methodology for off-line LDI-MS characterization of reactions that occurred on a levitated particle. (A) The levitation apparatus. (B) (i) Droplet generation and injection into the EDB, (ii) heterogeneous/multiphase reactions on the resultant levitated particle, (iii) extraction of the particle from the EDB and impact onto the deposition plate to enable subsequent LDI-TOF-MS analysis. (C) A brief summary of the heterogeneous/multiphase particle phase reactions. The (i) starting compounds and (ii) product compounds of the reactions. Note that only a small portion of the top-most region of the particle is depicted in panels (i) and (ii).

levitated, and characterize using LDI-TOF-MS the outcomes of the parallel condensation and reaction of these vapors on the particle.

2. Experiment

2.1. Chemicals

Reagent grade methanol, glycerol, sodium chloride, and nitric acid were purchased from BDH Inc. (Toronto, Ont., Can.). The sodium chloride used contained 0.01% bromide, 0.003% nitrate, 0.005%

potassium. Benzaldehyde and 1,8-diaminonaphthalene were purchased from Aldrich (Oakville, Ont., Can.).

2.2. Droplet dispensing and the electrodynamic balance

The droplet dispenser, the ring electrodes of the electrodynamic balance (EDB), and the substrate were enclosed in a plexiglass chamber (Fig. 1) (Bogan & Agnes, 2002). This chamber eliminated air convection in the laboratory from disturbing the trajectories of levitated objects.

The droplet dispenser used in this work was purchased from Uni-photon Systems (Brooklyn, NY, USA). Starting solutions were loaded into the internal reservoir using a micropipette. The droplet dispenser was equipped with a 40 μm diameter nozzle from which discrete 37 ± 3 μm radius droplets were produced as outlined here. A time variant waveform was applied to the piezoceramic element of the droplet dispenser that caused it to constrict, with the resultant pressure wave causing a volume of liquid to be ejected as a jet from the nozzle. During separation from the nozzle, the jet of liquid collapsed to form a single droplet. The nozzle of the droplet dispenser was positioned 1 mm from a plate electrode, and centered over a 5 mm diameter hole that had been cut in this electrode. A DC bias potential (0–250 V) was applied to this electrode. The electric field created by applying the DC potential on the plate induced charge separation in the jet, which resulted in each droplet having net charge. Hereafter, this electrode will be referred to as the induction electrode.

The EDB consisted of two 2 cm diameter ring electrodes that were fabricated from 1 mm diameter wire and mounted parallel at a separation distance of 8 mm. A 60 Hz sine wave ranging in amplitude from 500–3000 V_{0-P} was applied to the electrodes in phase. The two end cap electrodes consisted of the induction electrode and another flat plate as the top electrode. The top electrode was a stainless steel matrix assisted laser desorption/ionization (MALDI) sample platform, and it will be referred to hereafter as the deposition plate. During the droplet generation process, a sheath placed between the ring electrodes of the EDB and the deposition plate prevented unlevitated droplets from contaminating the deposition plate. The sheath was a piece of weighing paper. A DC potential was also applied to the stainless steel deposition plate. The operating characteristics of the EDB and the details of extracting a single levitated particle from the EDB and depositing it onto a deposition plate were reported elsewhere (Bogan & Agnes, 2002).

2.3. Levitated particles of user-defined composition

The volume of the initial droplet formed from this dispenser can be controlled through variation of the DC amplitude applied to the piezoelectric strips of the droplet dispenser, use of a different sized nozzle, or changing the composition of the starting solution. We have found it most practical to vary the concentration of dissolved solids or the amount of non-volatile solvent in the starting solution to vary the mass of non-volatile material in the levitated particle. The majority of the volatile solvent in the starting solution evaporated within a few seconds following the droplet formation event (Shulman, Charlson, & Davis, 1997), which left behind a residual droplet or particle.

Two starting solutions were used. For the studies involving the dispensing of droplets containing sodium chloride to create sodium chloride particles, the starting solution consisted of 3.0 M NaCl in distilled deionized water. The studies that involved the simultaneous organic and inorganic reaction monitoring were performed using a single starting solution that contained 0.25 M NaCl and 0.01 M

1,8-diaminonaphthalene in 80:20 water:methanol. The droplets/particles created from the latter starting solution each contained 1.6 pmol of 1,8-diaminonaphthalene, and the diameter of the resultant particles were typically 20 μm. A population of 20–30 particles/droplets was levitated in any one trial of an experiment.

2.4. Reactions on the levitated particles

Throughout, the relative humidity was monitored using a Traceable Digital Hygrometer/Thermometer (Control Company, Friendswood, TX). The environment in the levitation chamber was not controlled differentially from that in the laboratory. The relative humidity within the laboratory, and therefore also within the levitation chamber ranged from 15% to 35% dependent on the day in which the experiment was performed. Experiments were performed at relative humidity $< 35\%$ as to ensure particle formation (Choi & Chan, 2002). Given that imine formation occurs through a dehydration reaction, the presence of water on the particle may play a role in the reaction. However, Haddrell and Agnes (2004) have shown that imine formation can occur under conditions of elevated relative humidity ($> 60\%$) through a multiphase reaction. As such, the presence of water on the particle is believed to have a negligible effect on the rate of imine formation.

In all experiments the particles were levitated for 10 min prior to introducing reactive vapors. Nitric acid vapor was introduced to the chamber in which particles were levitated by simply placing into the chamber a 10 mL beaker containing 1 mL of concentrated nitric acid, resulting in a final concentration of nitric acid vapor of $\sim 79,000$ ppm. Haddrell and Agnes (2004) have shown previously that imine formation occurs under conditions of both low and high aldehyde concentrations. In experiments in which organic and inorganic reactions were allowed to proceed, two 10 mL beakers were placed inside the levitation chamber, one beaker contained 1 mL of concentrated nitric acid and the other 1 mL of benzaldehyde (gas phase concentration of benzaldehyde in the levitation chamber was ~ 170 ppm). The beakers were removed from the levitation chamber prior to depositing the droplets/particles onto the deposition plate. Each particle was deposited onto a separate location on the deposition plate, approximately 125 μm apart (Haddrell & Agnes, 2004).

2.5. Offline particle laser desorption ionization time-of-flight mass spectrometry

All mass spectra were collected after removing the deposition plate from the levitation chamber and inserting it into a Perspective Biosystems Voyager-DE matrix assisted laser desorption ionization TOF-MS (Framingham, MA, USA). The delay time between the particle deposition event and LDI-MS analysis ranged from 3 to 5 min. The output of the N_2 laser (337 nm) was attenuated using a variable density filter in the range from 331 to 763 μJ/pulse. The detection of the starting material, 1,8-diaminonaphthalene and its reaction products absorbed the 337 nm output of the N_2 laser, and hence their detection as molecular radical cations required relatively low laser pulse irradiance. Conversely, the detection of ionized salt clusters, by desorption ionization of the NaCl particles, required pulse irradiance energies > 550 μJ/pulse.

Haddrell and Agnes (2004) have shown that under similar conditions, with respect to time, humidity and temperature, the reactions between NaCl or 1,8-diaminonaphthalene with nitric acid or benzaldehyde, adsorbed onto the deposition plate during the period of droplet/particle levitation, were negligible relative to the quantity of product compounds that had formed on the levitated particle. To verify this in this work, unlevitated droplets were dispensed directly onto a remote location on the deposition plate immediately
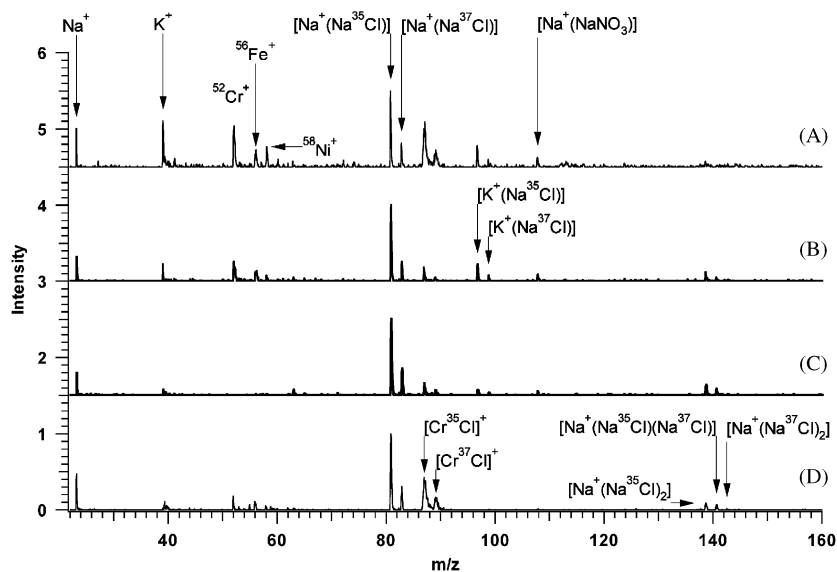
Fig. 2. The LDI-TOF mass spectra collected from a single NaCl particle that had been exposed to $HNO_{3(g)}$ for 1 h. The ion signal intensities in each mass spectrum were normalized to the $[Na^+(Na^{35}Cl)]$ peak. Each mass spectrum is the average of four consecutive laser pulses (A) 1–4, (B) 5–8, (C) 9–12, (D) 13–16. The laser irradiation energy was set to 644 μJ/pulse.

after the particle deposition. Upon mass spectral analysis, it was shown that imine production was not detectable on the deposition plate during the delay time (3–5 min).

3. Results

3.1. An inorganic multiphase/heterogeneous reaction

The results described in this section characterize the production of an inorganic compound on suspended particles, which later in this study will be built upon by introducing organic compounds to the system. NO_x emissions from high temperature combustion sources undergo oxidation to form HNO_3, which undergo further reactions on NaCl particles (Davies & Cox, 1998; de Haan & Finlayson-Pitts, 1997; Finlayson-Pitts, Ezell, & Pitts, 1989; Finlayson-Pitts & Hemminger, 2000; Foster et al., 2001; Knipping et al., 2000; Weis & Ewing, 1999). The anion exchange reaction that results in $NaNO_3$ production is indicated as Eq. (1) (Gard et al., 1998; Vogt, Crutzen, & Sander, 1996).

$$HNO_{3(g)} + NaCl_{(particle)} \rightarrow HCl_{(g)} + NaNO_{3(particle)}. \tag{1}$$

We proceeded to generate isolated NaCl particles that were then exposed to high concentrations of $HNO_{3(g)}$ for 1 h. In Fig. 2, four sequential LDI-TOF-MS spectra from one such particle are plotted. In acquiring that data, the irradiation energy of the laser and the position of the laser focus were not adjusted. Fig. 2A shows the ions detected from the first four laser shots fired at the particle. The expected ions of Na^+, $[Na^+(Na^{35}Cl)]$, and $[Na^+(Na^{37}Cl)]$ were detected, as was an ion signal indicative of a heterogeneous reaction product, $[Na^+(NaNO_3)]$. The surface specificity of the reaction (Carson, Johnston, & Wexler,

1997) and the analysis by LDI-TOF-MS, can be appreciated by comparison of the ion signal intensities in Fig. 2A to those in Fig. 2B–D. As the number of laser shots increased, the original surface material on the particle was removed, as indicated by the decrease in signal intensity of the cluster $[Na^+(NaNO_3)]$. Coinciding with this observation was the appearance of three new cluster ion peaks in Fig. 2B at $m/z = 139$, 141 and 143, corresponding to the isotopic distribution expected for chlorine in $[Na^+(NaCl)_2]$. The signal intensity of these ions increased with subsequent laser shots, suggesting that the ions observed in Fig. 2D originated from material representative of the NaCl particle core.

The ion peaks labeled as Na^+, K^+, $^{52}Cr^+$, $^{56}Fe^+$, and $^{58}Ni^+$ ions were background ions. These ions were also observed from the clean stainless steel plate using laser intensities $> 495 \, \mu J/pulse$ on the Perseptive Biosystems Voyager-DE. This grouping of background ions from a stainless steel plate has also been reported by Cody et al. who also irradiated a stainless steel plate with the output of a nitrogen laser (Cody et al., 1980). The ions at $m/z = 87$ and 89 are assigned as $[Cr^{+35}Cl]$ and $[Cr^{+37}Cl]$. The broad spectral width of these ion peaks suggests that these ions were formed by a different desorption/ionization mechanism than other ions in the spectrum.

Currently, the presence of potassium and sodium ions in the background hinders our ability to monitor their distribution within the particle. The ability to monitor this would be of interest as multicomponent aerosol crystallization creates particles that do not have homogeneous chemical morphology, and they often exhibit a surface layer enriched by minor components (Zhaozhu, Wexler, & Johnston, 1998a,b, 1996). Zhaozhu et al. have shown that the K^+/Na^+ peak area ratio observed in droplets created with identical NaCl and KCl mole fractions increased as the relative humidity increased, indicating that the surface properties of the aerosol particles could be quite different from the composition of the droplet's core (Zhaozhu et al., 1998a,b). The effect of the Na^+/K^+ signal intensity is but one aspect of the problem of matrix effects in quantitative analysis, and thus is proving a tremendous challenge in single particle analysis (Bate, Leake, Matthews, & Wallach, 1993; Cooks & Busch, 1983; Gross, Galli, Silva, & Prather, 2000; Kane & Johnston, 2000; Olesik, 1997; Schoolcraft, Constable, Zhigilei, & Garrison, 2000; Woods, Smith, Dessiaterik, Baer, & Miller, 2001; Xu, Balik, & Agnes, 2001; Zhaozhu et al., 1998a,b, 1996). The capability to obtain multiple samplings from a single particle may allow a profile of a particle's morphology, and possibly a better understanding of the matrix effects.

3.2. Simultaneous inorganic and organic reactions

Having characterized the production of $NaNO_3$, the complexity of the system was incremented by the introduction of organic compounds. A population of particles created using the starting solution containing 0.01 M 1,8-diaminonaphthalene and 0.25 M NaCl in distilled deionized water were dispensed, and levitated. Benzaldehyde and nitric acid were then introduced, in separate reservoirs, to the levitation chamber. The 1,8-diaminonaphthalene reacts with aldehydes by way of a dehydration reaction to form an imine (Haddrell & Agnes, 2004). After a 40 min levitation period, the nitric acid and benzaldehyde were removed from the chamber and the levitated particles were then deposited onto the deposition plate.

One of these particles was characterized by LDI-TOF-MS using the following procedure. First, the laser output was centered over the deposited salt particle. The laser irradiation energy was set to $467 \, \mu J/pulse$ and the ions detected from firing the laser 8 times were summed and then the average ion signal plotted as the mass spectrum identified as Fig. 3A. The laser was then fired at the salt particle at that laser irradiation energy until no further ion signals were detected (typically 100–150 laser shots), at which point, the laser irradiation energy was incremented by $27 \, \mu J/pulse$, and another mass spectrum from the first 8 laser
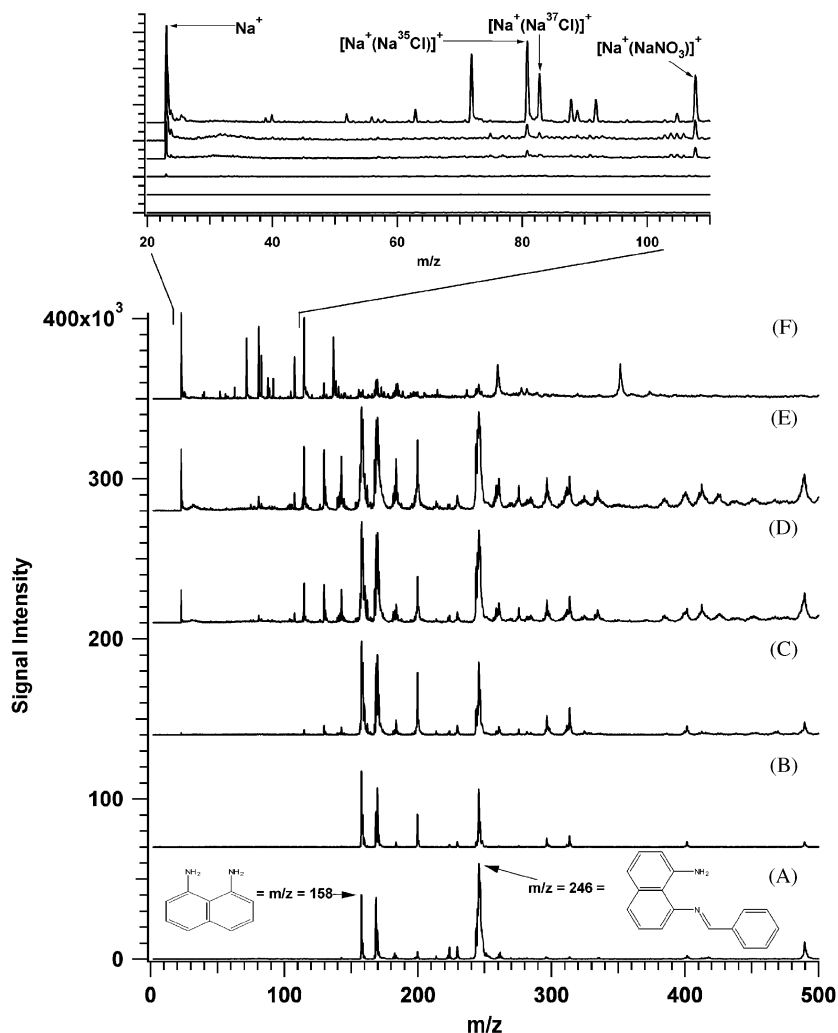
Fig. 3. LDI-TOF mass spectra collected from a single NaCl particle dosed with 1.6 pmol of 1,8-diaminonaphthalene that had been exposed to both nitric acid vapor and benzaldehyde vapor for 40 min. The laser irradiation energies used were (A) 467 (B) 493 (C) 537 (D) 556 (E) 585 (F) 614 μJ/pulse. Each mass spectrum is the average of first eight consecutive laser shots at each laser irradiation energy setting.

shots was acquired. This cycle was repeated until the laser irradiation energy reached $556\,\mu J$/pulse, at which point, ionized clusters of the inorganic compounds in the particle were detected, including a peak indicative of the inorganic heterogeneous reaction product, $[Na^+(NaNO_3)]$. Fig. 3D and E contain the ion signals of both the starting materials and products of the inorganic and organic heterogeneous/multiphase reactions. In Fig. 3F there were no ion signals indicative of the reaction between 1,8-diaminonaphthalene and benzaldehyde, suggesting that the organic species had been desorbed from the particle surface by the preceding laser shots.
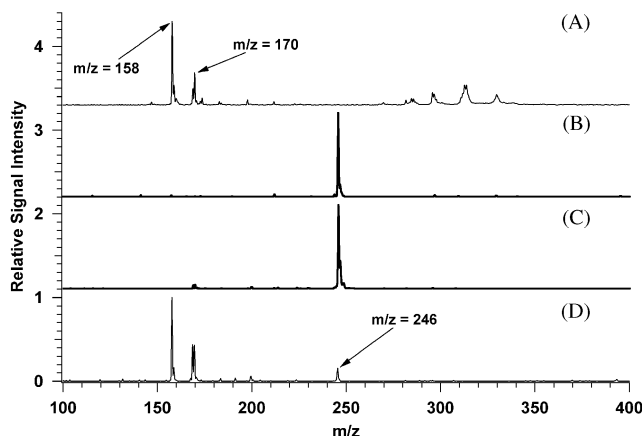
Fig. 4. LDI-TOF mass spectra collected from four different salt particles, each dosed with 1.6 pmol of 1,8-diaminonaphthalene, that were levitated in a chamber under four different conditions. (A) Pure, unlevitated starting material that had been passed through the droplet dispenser. (B) 1 mL of pure benzaldehyde and nitric acid were introduced into the chamber simultaneously. (C) 1 mL of pure benzaldehyde was introduced into the chamber for a period of 45 min, then the benzaldehyde was removed and 1 mL of nitric acid was placed into the chamber for 55 min. (D) 1 mL of nitric acid was placed into the chamber for 2 h, after which time, 1 mL of benzaldehyde was introduced into the chamber for 1 h (note that the nitric acid remained in the chamber for 3 h). The laser irradiation energies used for the four trials were as follows: (A) 440 μJ/pulse, (B) 413 μJ/pulse, (C) 440 μJ/pulse and (D) 614 μJ/pulse. Each spectrum is an average of eight consecutive laser pulses.

3.3. Effect of the sequence of reactant addition on imine formation

Having established that the simultaneous introduction of nitric acid and benzaldehyde vapor does not prevent the imine reaction from proceeding, the order in which the two reactants were added to the chamber on the outcome of imine formation was investigated.

A blank, in which a population of particles was levitated for 30 min without the addition of beakers containing nitric acid or benzaldehyde was performed. A mass spectrum from the LDI-TOF-MS characterization of one of the particles at a laser irradiation energy of 440 μJ/pulse allowed detection of the starting material, 1,8-diaminonaphthalene as its radical cation, and an imine resultant from its reaction with ambient formaldehyde that was present in the air in the laboratory (Fig. 4A).

In the first iteration, both nitric acid and benzaldehyde were simultaneously placed into separate reservoirs within the levitation chamber containing a population of levitated particles. Following a 30-min levitation/reaction exposure period, the particles were deposited and analyzed via LDI-TOF-MS. As shown in the mass spectrum identified as Fig. 4B, an ion signal indicative of the imine product at $m/z = 246$ was detected. Equilibrium vapor pressures for benzaldehyde and nitric acid were 1.7×10^{-4}, and 7.9×10^{-2} atm, respectively. As such, the nitric acid concentration in the gas phase was higher than that of benzaldehyde over the course of the reaction, yet there appeared little inhibition of the imine formation in this experiment.

In the second iteration, a population of droplets dosed with 1,8-diaminonaphthalene was injected into the EDB and levitated prior to introducing 1 mL of benzaldehyde into the levitation chamber. After 45 min, the beaker containing the benzaldehyde was removed and 1 mL of nitric acid in a different beaker was introduced to the chamber. After an additional period of 55 min, the particles were deposited and analyzed via LDI-TOF-MS (Fig. 4C). From a relatively low laser pulse energy of 440 μJ/pulse, no ion signal for
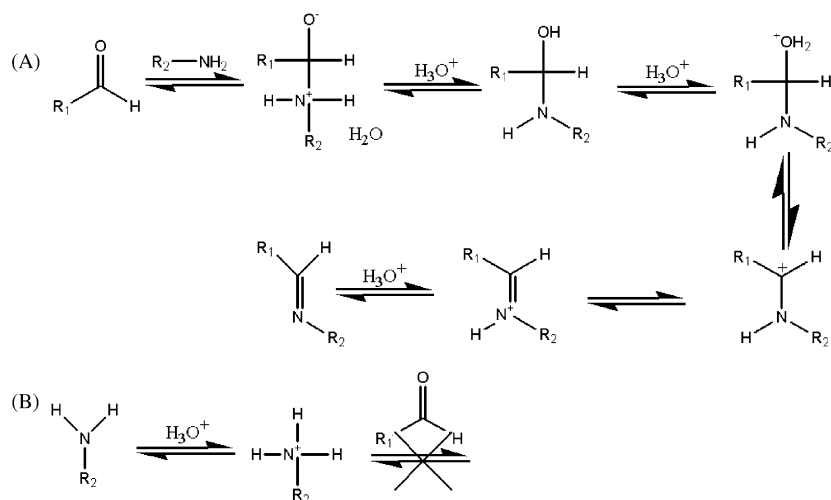
Fig. 5. The reaction mechanism of imine formation, dependent on whether acid was added to the system (A) after or (B) before the introduction of the aldehyde.

the starting material was detected, yet a large ion signal of the product ($m/z = 246$) was observed. This indicates that the nitric acid did not break down the imine once it had formed suggesting that the imine reaction was not reversible at these conditions. As such, the imines formed by such reactions could have lifetimes longer than an initial estimate of ~ 6 h (Haddrell & Agnes, 2004).

In the final run, a population of salt particles plus 1,8-diaminonaphthalene was levitated, with 1 mL of pure nitric acid in a reservoir placed within the chamber. After 2 h, the nitric acid was removed and 1 mL benzaldehyde in a separate reservoir was placed within the chamber. After 1 h, the particles were deposited and analyzed via LDI-TOF-MS (Fig. 4D). The ion signal of the product imine at $m/z = 246$ was detected, but note that a very high laser irradiation energy (614 μJ/pulse) was necessary in order to observe this ion (no ion signal indicative of the imine product was observed at a laser irradiation energy of 440 μJ/pulse). This indicates that the amount of the imine formed during the course of this levitation period was greatly reduced. To understand this result, the reaction mechanism for the formation of an imine must be considered (Fig. 5). The highest rate of imine formation occurs in a pH range between 4 and 5 (Jencks, 1959; Lowry & Richardson, 1976). The rate-determining step of the reaction is the initial attack of the lone pair electrons of the amine on the carbonyl carbon of the aldehyde, followed by stabilization of that intermediate by the introduction of an electron acceptor. However, the exposure of the amine to nitric acid was found to significantly decrease the rate of imine formation. The reduction in imine formation can be attributed to the fact that the nitric acid vapor was given sufficient time to interact with the levitated particles containing 1,8-diaminonaphthalene prior to the introduction of the benzaldehyde vapor. The results presented also indicate that the protonation of the reactant 1,8-diaminonaphthalene by the uptake of HNO$_3$ under the conditions studied was irreversible. As indicated by the reaction scheme in Fig. 5B, the nitric acid protonates the primary amine, effectively preventing the lone pair on the N atom of the amine group from attacking the carbonyl carbon. Although 1,8-diaminonaphthalene has two amine groups, protonation of both groups may not be required to significantly decrease the rate of imine formation as the two amine groups are conjugated, and as such a positive charge on one of the amines will alter the basicity of the other.

4. Discussion

The laser irradiation energy that was used to acquire each mass spectrum needs consideration when interpreting the LDI-TOF-MS data. For instance, both spectra indentified as Figs. 3A and 4B were obtained from similarly produced particles. Differences in the spectra, such as the detection of the starting compound, 1,8-diaminonaphthalene (molecular radical cation at $m/z = 158$) was due to differences in the laser irradiation energies used during sample characterization. Another example of this is evident in the decreased imine abundance, relative to the ion signals of the starting reactants, detected from a particle that had been first exposed to nitric acid (compare ion signal intensity at $m/z = 246$ in Fig. 4A versus Fig. 4D). The relatively low ion signal intensity of the imine's radical cation (Fig. 4D), coupled with the high laser irradiation energy required to generate those ion signals, indicates that its production was relatively slow during the levitation period.

A feature of the methodology used to acquire the mass spectra reported herein is that each particle levitated in the EDB can be viewed as an individual reaction vessel. Here, LDI mass spectral analysis was carried out on each individual particle, but other instrumental methods, such as force microscopy (Lehmpuhl, Ramirez-Aguilar, Michel, Rowlen, & Birks, 1999) and optical microscopy could each be invoked to provide complementary, or new data. We anticipate that this strategy can be used as a platform with which standard analytical methodologies can be implemented for improved quantitative compound characterization of individual particles. The use of femtosecond laser pulses (Smith et al., 1998) could allow for increased specificity for the characterization of a particle's surface composition. Such a platform can also be used to develop models to account for chemical composition evolution of individual particles in a tropospheric airmass. The potential for this was demonstrated through the differential production of the imine by variation of the order of introduction of nitric acid versus aldehyde vapor to the levitation chamber. This could be the most significant finding in this study and it best exemplifies why methodology capable of monitoring simultaneously occurring organic and inorganic particle-phase reactions is necessary. Thus, not only do the relative rates of a reaction need to be considered, but the particle's history and local environment also needs to be considered.

Currently, the simultaneous monitoring of organic and inorganic homogeneous/heterogeneous/multiphase reactions described here is qualitative, though standard quantitation strategies can be incorporated into the method to enable semi-quantitative results (Haddrell & Agnes, 2004). Nevertheless, the methodology described herein is a step toward understanding, and possibly monitoring of the rates of inorganic and organic reactions occurring simultaneously on suspended particles in the troposphere.

Acknowledgements

References

Aardahl, C. L., Vehring, R., Davis, E. J., Schweiger, G., & Swanson, B. D. (1997). Trapping two-particle arrays in a double ring electrodynamic balance. *Journal of Aerosol Science*, *28*, 1491–1505.

Adamson, I. Y., Prieditis, H., & Vincent, R. (1999). Pulmonary toxicity of an atmospheric particulate sample is due to the soluble fraction. *Toxicology and Applied Pharmacology*, *157*, 43–50.

Bate, D., Leake, J., Matthews, L., & Wallach, E. (1993). Matrix effects on the relative sensitivity factors measured by laser microprobe mass spectrometry. *International Journal of Mass Spectrometry and Ion Processes*, *127*, 85–93.

Bogan, M. J., & Agnes, G. R. (2002). MALDI-TOF-MS analysis of droplets prepared in an electrodynamic balance: "wall-less" sample preparation. *Analytical Chemistry*, *74*, 489–496.

Brook, R. D., Franklin, B., Cascio, W., Hong, Y., Howard, G. H., Lipsett, M., Luepker, R., Mittleman, M., Samet, J., Smith, S. C., & Tager, I. (2004). Air pollution and cardiovascular disease. *Circulation*, *109*, 2655–2671.

Carson, P. G., Johnston, M. V., & Wexler, A. S. (1997). Real-time monitoring of the surface and total composition of aerosol particles. *Journal of Aerosol Science*, *26*, 291–300.

Choi, M. Y., & Chan, C. K. (2002). The effects of organic species on the hygroscopic behaviors of inorganic aerosols. *Environmental Science and Technology*, *36*, 2422–2428.

Cody, R. B., Burnier, R. C., Reents, W. D., Carlin, T. J., McCrery, R. K., Lengel, R. K., & Freiser, B. S. (1980). Laser ionization source for ion cyclotron resonance spectroscopy. Application to atomic metal ion chemistry. *International Journal of Mass Spectrometry and Ion Physics*, *33*, 37–43.

Cooks, R. G., & Busch, K. L. (1983). Matrix effects, internal energies and MS/MS spectra of molecular ions sputtered from surfaces. *International Journal of Mass Spectrometry and Ion Physics*, *53*, 111–124.

Davis, E. J. (1997). A history of single aerosol particle levitation. *Aerosol Science and Technology*, *26*, 212–254.

Davies, J. A., & Cox, R. A. (1998). Kinetics of the heterogeneous reaction of HNO_3 with NaCl: effect of water vapor. *Journal of Physical Chemistry A*, *102*, 7631–7642.

de Haan, D. O., & Finlayson-Pitts, B. J. (1997). Knudsen cell studies of the reaction of gaseous nitric acid with synthetic sea salt at 298 K. *Journal of Physical Chemistry A*, *101*, 9993–9999.

Dockery, D. W., Pope, C. A., & Xu, X. (1993). An association between air pollution and mortality in six US cities. *New England Journal of Medicine*, *329*, 1753–1759.

Finlayson-Pitts, B. J., Ezell, M. J., & Pitts, J. N. (1989). Formation of chemically active chlorine compounds by reaction of atmospheric NaCl particles with gaseous N_2O_5 and $ClONO_2$. *Nature*, *337*, 241–244.

Finlayson-Pitts, B. J., & Hemminger, J. C. (2000). Physical chemistry of airborne sea salt particles and their components. *Journal of Physical Chemistry A*, *104*, 11463–11477.

Finlayson-Pitts, B. J., & Pitts, J. N. (1997). Tropospheric air pollution: ozone, airborne toxics, polycyclic hydrocarbons, and particles. *Science*, *276*, 1045–1052.

Foster, K. L., Plastridge, R. A., Bottenheim, J. W., Shepson, P. B., Finlayson-Pitts, B. J., & Spicer, C. W. (2001). The role of Br_2 and BrCl in surface ozone destruction at polar sunrise. *Science*, *291*, 471–474.

Gard, E. E., Kleeman, M. J., Gross, D. S., Hughes, L. S., Allen, J. O., Morrical, B. D., Fergenson, D. P., Dienes, T., Galli, M. E., Johnson, R. J., Cass, G. R., & Prather, K. A. (1998). Direct observation of heterogeneous chemistry in the atmosphere. *Science*, *279*, 1184–1187.

Gross, D. S., Galli, M. E., Silva, P. J., & Prather, K. A. (2000). Relative sensitivity factors for alkali metal and ammonium cations in single-particle aerosol time-of-flight mass spectra. *Analytical Chemistry*, *72*, 416–422.

Haddrell, A. E., & Agnes, G. R. (2004). A class of heterogeneous/multiphase organic reactions studied on droplets/particles levitated in a laboratory environment: aldehyde + 1,8-diaminonaphthalene = imine. *Atmospheric Environment*, *38*, 545–556.

Jang, M., Czoschke, N. M., Lee, S., & Kamens, R. (2002). Heterogeneous atmospheric aerosol production by acid-catalyzed particle-phase reactions. *Science*, *298*, 814–817.

Jencks, W. P. (1959). Studies on the mechanism of oxime and semicarbazone formation. *Journal of the American Chemical Society*, *81*, 475.

Kalberer, M., Paulsen, D., Steinbacher, M., Dommen, J., Prevot, A. S. H., Fisseha, R., Weingartner, E., Frankevich, V., Zenobi, R., & Baltensperger, U. (2004). Identification of polymers as major components of atmospheric organic aerosols. *Science*, *303*, 1659–1662.

Kane, D. B., & Johnston, M. V. (2000). Size and composition biases on the detection of individual ultrafine particles by aerosol mass spectrometry. *Environmental Science and Technology*, *34*, 4887–4893.

Knipping, E. M., Lakin, M. J., Foster, K. L., Jungwirth, P., Tobias, D. J., Gerber, R. B., Dabdub, D., & Finlayson-Pitts, B. J. (2000). Experiments and simulations of ion-enhanced interfacial chemistry on aqueous NaCl aerosols. *Science*, *288*, 301–306.

Lehmpuhl, D. L., Ramirez-Aguilar, K. A., Michel, A. E., Rowlen, K. L., & Birks, J. W. (1999). Physical and chemical characterization of atmospheric aerosols by atomic force microscopy. *Analytical Chemistry*, *71*, 379–383.

Lowry, T. H., & Richardson, K. S. (1976). *Mechanism and Theory in Organic Chemistry* (1st ed.). New York: Harper & Row.

Olesik, J. W. (1997). Investigating the fate of individual sample droplets in inductively coupled plasmas. *Applied Spectroscopy*, *51*, 158A–175A.

Pope, C. A. I., Thun, M. J., Namboodiri, M. M., Dockery, D. W., Evans, J. S., Speizer, F. F., & Clarke, C. W. J. (1995). Particulate air pollution as a predictor of mortality in a prospective study of US adults. *American Journal of Respiratory and Critical Care Medicine*, *151*, 669–674.

Ravishankara, A. R. (1997). Heterogeneous and multiphase chemistry in the troposphere. *Science*, *276*, 1058–1065.

Salvi, S., & Holgate, T. (1999). Mechanisms of particulate matter toxicity. *Clinical and Experimental Allergy*, *29*, 1187–1194.

Samet, J. M., Dominici, F., Curriero, F. C., Coursac, I., & Zeger, S. L. (2000). Fine particulate air pollution and mortality in 20 US cities, 1987–1994. *New England Journal of Medicine*, *343*, 1742–1749.

Schoolcraft, T. A., Constable, G. S., Zhigilei, L. V., & Garrison, B. J. (2000). Molecular dynamics simulation of the laser disintegration of aerosol particles. *Analytical Chemistry*, *72*, 5143–5150.

Schweiger, G., & Davis, E. J. (2002). The Airborne Microparticle. Heidelberg: Springer.

Shulman, M. L., Charlson, R. J., & Davis, E. J. (1997). The effects of atmospheric organics on aqueous droplet evaporation. *Journal of Aerosol Science*, *28*, 737–752.

Smith, D. J., Ledingham, K. W. D., Singhal, R. P., Kilic, H. S., McCanny, T., Langley, A. J., Taday, P. F., & Kosmidis, C. (1998). Time-of-flight mass spectrometry of aromatic molecules subjected to high intensity laser beams. *Rapid Communications in Mass Spectrometry*, *12*, 813–820.

Somers, C., McCarry, B. E., Malek, F., & Quinn, J. S. (2004). Reduction of particulate air pollution lowers the risk of heritable mutations in mice. *Science*, *304*, 1008–1010.

Tan, W. C., Qui, D., Liam, B. L., Lee, S. H., Van Eeden, S. F., D'yachkova, Y., & Hogg, J. C. (2000). The human bone marrow response to fine particulate air pollution. *American Journal of Respiratory and Critical Care Medicine*, *161*, 1213–1217.

van Eeden, S. F., Tan, W. C., Suwa, T., Mukae, H., Terashima, T., Fujii, T., Qui, D., Vincent, R., & Hogg, J. C. (2001). Cytokines involved in the systemic inflammatory response induced by exposure to particulate matter air pollutants (PM10). *American Journal of Respiratory and Critical Care Medicine*, *164*, 1–5.

Vehring, R., Aardahl, C. L., Davis, E. J., Schweiger, G., & Covert, D. S. (1997). Electrodynamic trapping and manipulation of particle clouds. *Review of Scientific Instruments*, *68*, 70–78.

Vincent, R., Bjarnason, S. G., Adamson, I. Y., Hedgecock, C., Kumarathasan, P., Guenette, J., Potvin, M., Goegan, P., & Bouthillier, L. (1997). Acute pulmonary toxicity of urban particulate matter and ozone. *American Journal of Pathology*, *151*, 1563–1570.

Vogt, R., Crutzen, P. J., & Sander, R. (1996). A mechanism for halogen release from sea-salt aerosol in the remote marine boundary layer. *Nature*, *383*, 327–330.

Weis, D. D., & Ewing, G. E. (1999). The reaction of nitrogen dioxide with sea salt aerosol. *Journal of Physical Chemistry A*, *103*, 4865–4873.

Willerson, J. T., & Ridker, P. M. (2004). Inflammation as a cardiovascular risk factor. *Circulation*, *109*, II-2–II-10.

Woods, E., Smith, G. D., Dessiaterik, Y., Baer, T., & Miller, R. E. (2001). Quantitative detection of aromatic compounds in single aerosol particle mass spectrometry. *Analytical Chemistry*, *73*, 2317–2322.

Wuerker, R. F., Shelton, H., & Langmuir, R. V. (1959). Electrodynamic containment of charged particles. *Journal of Applied Physics*, *30*, 342.

Xu, J. Q., Balik, D., & Agnes, G. R. (2001). Aerosol static electrification and its effect in inductively coupled plasma spectroscopy. *Journal of Analytical Atomic Spectrometry*, *16*, 715–723.

Zenobi, R., Haefliger, O., & Bucheli, T. (2000). Laser mass spectrometric analysis of organic atmospheric aerosols. 2. Elucidation of urban air pollution processes. *Environmental Science and Technology*, *34*, 2184–2189.

Zhaozhu, G., Wexler, A. S., & Johnston, M. V. (1996). Multicomponent aerosol crystallization. *Journal of Colloid Interface Science*, *183*, 68–77.

Zhaozhu, G., Wexler, A. S., & Johnston, M. V. (1998a). Deliquescence bahavior of multicomponent aerosols. *Journal of Physical Chemistry A*, *102*, 173–180.

Zhaozhu, G., Wexler, A. S., & Johnston, M. V. (1998b). Laser desorption/ionization of single ultrafine multicomponent aerosols. *Environmental Science and Technology*, *32*, 3218–3223.